Processing and Application of Ceramics 9 [4] (2015) 215–223
DOI: 10.2298/PAC1504215S

Crystallization and thermo-mechanical properties of Li_2O-ZnO-CaO-SiO_2 glass-ceramics with In_2O_3 and Fe_2O_3 additives

Saad M. Salman, Samia N. Salama, Ebrahim A. Mahdy*

Glass Research Department, National Research Centre, Dokki, Cairo, Egypt

Received 3 November 2015; Received in revised form 29 December 2015; Accepted 31 December 2015

Abstract

Li_2O-ZnO-CaO-SiO_2 based glasses were prepared by the conventional melting technique and subsequently converted to glass-ceramics by controlled crystallization. The nucleation and crystallization temperatures were determined by differential thermal analysis (DTA). The effects of adding In_2O_3 and Fe_2O_3 addition on the crystallization behaviour and thermo-mechanical properties of the prepared glass-ceramics were investigated. A study on the microstructure, close to the internal phases of the resulting glass-ceramics, was followed by using scanning electron microscope (SEM). The dilatometric thermal expansion and Vickers' microhardness of the crystalline products were also evaluated. The crystalline phases that can be found in the resulting glass-ceramics, identified by X-ray diffraction (XRD) analysis, are α-quartz-[SiO_2], lithium zinc silicate-[Li_2ZnSiO_4], lithium disilicate-[$Li_2Si_2O_5$], wollastonite-[$CaSiO_3$], wollastonite containing iron, ferrobustamite-[$(Ca_{0.79}Fe_{0.21})SiO_3$], and lithium indium silicate of pyroxene type-[$LiInSi_2O_6$]. Average thermal expansion coefficient (in the temperature range 25–700 °C) decreased from 191×10^{-7} 1/°C to 115×10^{-7} 1/°C and the Vickers' microhardness increased from 3.56 to 5.44 GPa with the increase of In_2O_3 and Fe_2O_3 contents in the glass-ceramics. The changes in the obtained expansion coefficient and microhardness were due to the formation of different phases which in turn influenced the rigidity/bonding and microstructure in the resultant glass-ceramics.

Keywords: *lithium zinc calcium silicate glass-ceramics, microstructure, hardness, thermal expansion*

I. Introduction

Glass-ceramics are the micro- or nanocrystalline materials produced by controlling crystallization of glasses [1], in which the crystalline phases are nucleated and grown in glass via heat treatment [2]. It is believed that the first stage in glass-ceramic formation is generally an amorphous phase separation as a result of micro- or nano-scale immiscibility in glass, with subsequent growth occurring in these regions [1]. The properties of glass-ceramics depend on the type and amount of the crystalline phases present, as well as the composition of the glassy matrix [3]. The ability to control these two parameters depends on the original composition and the heat-treatment regime [4]. Glass-ceramics show favourable chemical, thermal, dielectric and biological properties superior to metals and various polymers. Furthermore, they are superior to normal glasses and conventional ceramics as well, especially in their tuneable thermo-physical properties and microstructure [4].

Glass-ceramics from the lithium zinc silicate, LZS, system are a versatile class of material. There have been thoroughly studied not only because it can be prepared with a wide range of thermal expansion coefficients by controlling heat treatments [5], but also because some compositions within this system can yield useful glass-ceramics, in which orthosilicate can be crystallized. In this system, the study of the effect of substitutions with different cations can throw considerable light on the crystallization behaviour, formation of stable and metastable phases and compatibility relations between the different phases [6]. A number of studies have been carried out on the crystallization behaviour and thermo-physical properties of this system [7–10]. The influence of K_2O and P_2O_5 on crystallization sequence of Li_2O-ZnO-SiO_2 glass-ceramics containing low ZnO content was investigated by Chen and McMillan [9]. They confirmed that a small amount of

* Corresponding author: tel: +201068704325,
fax: +201068202333, e-mail: *emahdy10@yahoo.com*

K_2O changed the crystallization sequence and the phase composition of resulting glass-ceramics, while P_2O_5 produced a glass-ceramics with fine grained interlocking microstructures. West and Glasser [7] reported that, the introduction of calcium in Li_2O-ZnO-SiO_2 glass-ceramics at the expense of ZnO led to the formation of calcium monosilicate-wollastonite phase together with mixed phases of orthosilicate. Sharma *et al.* [11] investigated LZS glass-ceramics and showed that their thermophysical properties depend on the crystalline phases, like cristobalite, $Li_3Zn_{0.5}SiO_4$ and Li_2SiO_3, formed during the conversion of glass to glass-ceramic. With increasing the ZnO/(ZnO+SiO_2) ratio in the glass, higher amount of cristobalite and $Li_3Zn_{0.5}SiO_4$ and smaller amount of Li_2SiO_3 were formed in the glass-ceramics.

The glass-ceramics of LZS system have been applied in the fabrication of hermetic glass-ceramic to metal (GCM) seals [6,12] because of their tunable thermal expansion characteristics. James [13] also maintained that these materials can be used in the manufacture of hermetic seals to nickel-base super alloys.

Crystallization behaviour and properties of the lithium zinc silicates system with some trivalent oxides were studied by many authors [14–17]. However, there is no available data about the role of In_2O_3 and Fe_2O_3 and their influence on properties of the Li_2O-ZnO-SiO_2 glass-ceramics. With this motivation, the present work aimed to investigate the role of the addition of In_2O_3 and Fe_2O_3 on the crystallization behaviour and the types of crystalline phases formed by thermally treated lithium zinc calcium silicate glass. Thermal expansion coefficients and hardness values of the resultant glass-ceramics were also evaluated.

II. Experimental

2.1. Batch composition and glass preparation

The glass samples, presented in Table 1, were prepared by a conventional melting technique from high-purity chemicals (Fluka, ≥98% pure): Li_2CO_3, $CaCO_3$, ZnO, SiO_2, In_2O_3 and Fe_2O_3. Batches were thoroughly mixed and melted in Pt–2% Rh crucible in an electric furnace with SiC heating elements at 1300–1350 °C for 3 h. Melting was continued until clear homogeneous melt was obtained; this was achieved by swirling the melt several times at about 30 min intervals. The melts were cast in warm stainless steel molds into rods and buttons shape. The prepared samples were immediately transferred to an annealing muffle furnace regulated at 450 °C. The furnace was switched off after 1 h and left to cool down to room temperature to minimize the strain of the prepared glasses.

2.2. Crystallization and glass-ceramic formation

Differential thermal analysis (DTA) was employed for recording the glass transition temperature (T_g) and crystallization temperature (T_c) for all glass samples. Based on the DTA results, the controlled heat-treatment was applied for each glass with the goal to obtain glass-ceramic materials of holocrystalline mass with minimum residual glassy phase and without deformation. Therefore, double stage heat-treatment regimes, were used for crystallization. The glasses were first heat treated in a muffle furnace at endothermic temperature of each glass composition - the glass sample was soaked for 5 h to provide sufficient nucleation sites. The temperature was then raised to the exothermic temperature, specific for each glass for 10 h. A heating rate of 10 °C/min was used during the double stage heat-treatment regimes.

2.3. Characterization

A differential thermal analyser (SDTQ600-TA Instruments, USA) was employed for recording the glass transition temperature (T_g) and crystallization temperature (T_c). Measurements were done in the temperature range of 25–1000 °C using a heating rate of 10 °C/min from ambient temperature to 1000 °C in a flowing high purity nitrogen environment. The cast glass was crushed and sieved in 90–125 μm to produce (30 g) glass powder suitable for DTA measurement.

Identification of various crystalline phases in glass-ceramic samples were carried out using powder X-ray diffractometer (PW 1830; PANalytical) with Ni filtered Cu-Kα radiation, 2θ range from 5° to 80° range and scanning speed of 2°/min. The crystalline phases were identified by matching the peak positions of the intense peaks with PCPDF standard cards.

The fractured surfaces of the glass-ceramic samples were examined by scanning electron microscope (JEOL type JXA-840A Electron Probe Microanalyzer operated at 30 kV). The fractured surface of the samples was eroded with 1% (HF+HNO_3) solution for 60 s, and then sputtered with gold.

The thermal expansion coefficients (α) of the crystalline samples were measured by using a thermo-

Table 1. Chemical composition of the glass batches

Sample	Oxide contents [mol%]					
	Li_2O	ZnO	CaO	SiO_2	In_2O_3	Fe_2O_3
G_1	18.46	12.72	12.18	56.64	-	-
G_2	18.42	12.67	12.16	56.55	0.20	-
G_3	18.36	12.62	12.11	56.3	0.61	-
G_4	18.28	12.56	12.06	56.09	1.01	-
G_5	18.09	12.44	11.94	55.49	1.00	1.04
G_6	17.97	12.34	11.85	55.12	0.99	1.73

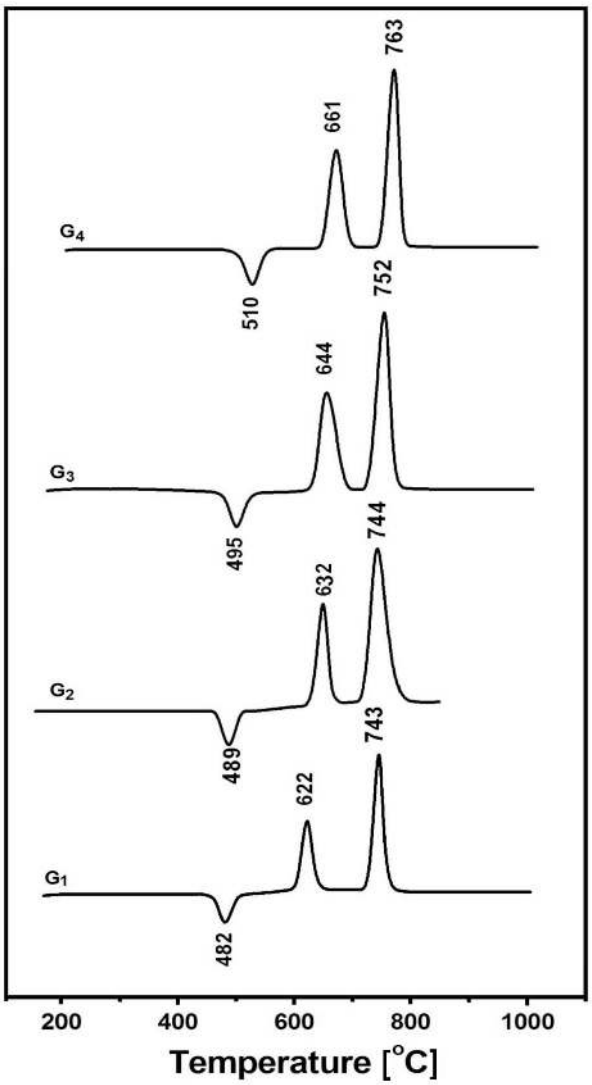

Figure 1. DTA data of the investigated glasses (G_1–G_4)

mechanical analyser (NETZSCH DIL402PC) in the temperature range 25–700 °C with a heating rate of 5 °C/min using silica probe. The linear thermal expansion coefficient (α) was automatically calculated using the general equation: $\alpha = (\Delta L/L) \cdot (1/\Delta T)$; where: ΔL is the increase in length, L is the original length of the specimen and ΔT is the temperature interval over which the sample is heated.

A microhardness tester (Shimadzu, Type-HMV, Japan) with applying loads of 100 g for 15 s was used to carry out the Vickers' microhardness measurements of the glass-ceramic samples. The samples were cut using a low speed diamond saw after controlled heat treatment, the specimens were carefully polished using 500, 800, and 1000 grit SiC paper and 3 and 1 mm diamond paste to obtain smooth and flat parallel surface glass-ceramic samples before indentation. At least 10 indentation readings for each sample were tested to get average value.

III. Results

3.1. Crystallization behaviour

The glass transition (T_g) and crystallization temperature (T_c) of each glass sample, deduced from the DTA results of each glass powder, are present in Figs. 1 and 2. The glass samples have a single endothermic dip before the onset of crystallization, which corresponds to the T_g with the inflection point situated between 482 and 510 °C. The exothermic peaks corresponding to the crystallization temperature (T_c) are observed in the temperature range 622–763 °C which indicates that the crystallization reaction takes place in the glass. From the DTA thermographs (Fig. 1), the additions of In_2O_3 in the base glass composition led to increase the temperatures which are needed to start the nucleation stage and crystal growth. While, the additions of iron oxide in In_2O_3-containing glass (Fig, 2), led to shift the endothermic and exothermic dips to lower temperatures i.e. a lower energy is needed to obtain crystallization in the glasses.

The X-ray diffraction patterns of the thermally treated glasses are presented in Figs. 3 and 4. The XRD analysis of the base glass G_1 crystallized at 480° °C/5 h–

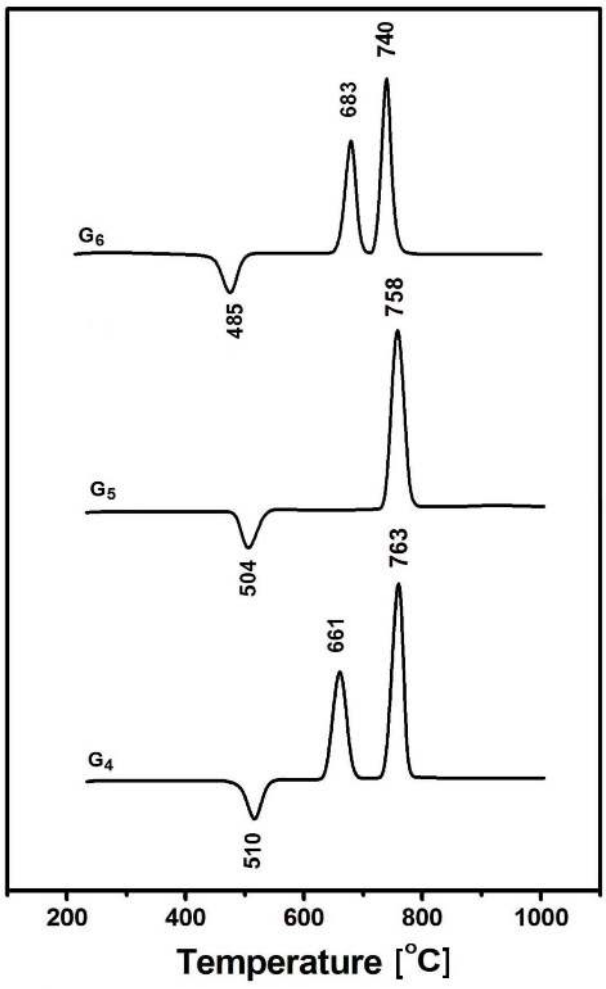

Figure 2. DTA data of the investigated glasses (G_4–G_6)

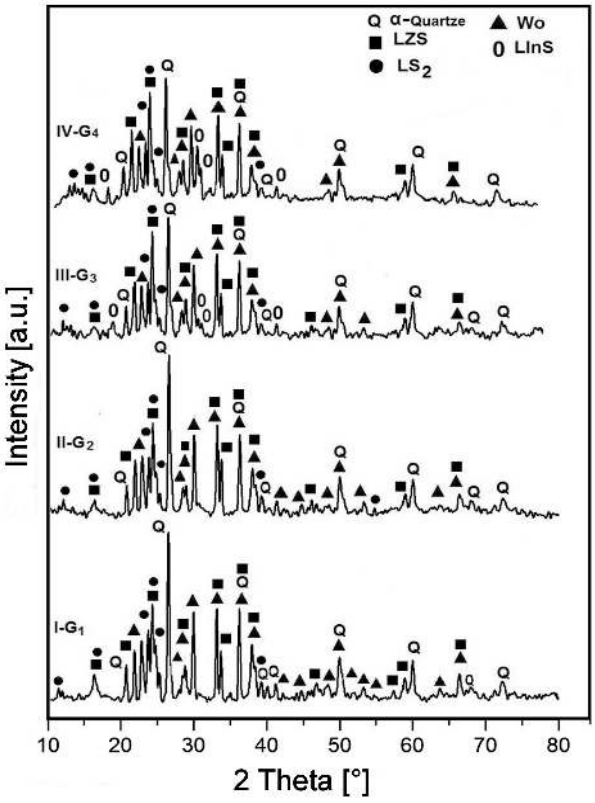

Figure 3. X-ray diffraction analysis of the crystallized glasses (G_1–G_4)

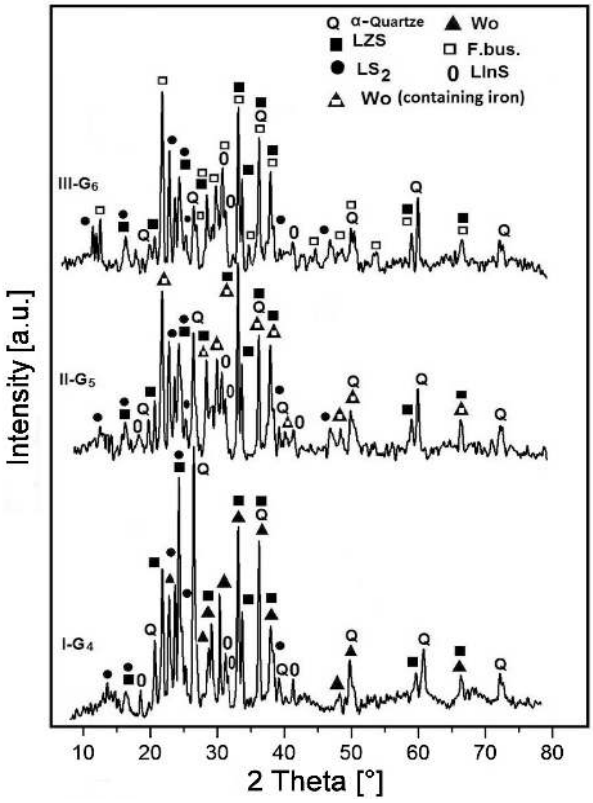

Figure 4. X-ray diffraction analysis of the crystallized glasses (G_4–G_6)

745 °C/10 h (Fig. 3, pattern I, Table 2), showed that α-quartz (SiO_2, Card No. 33-1161) crystallized together with lithium disilicate ($Li_2Si_2O_5$, Card No. 17-0447), wollastonite ($CaSiO_3$, Card No. 29-0372), and lithium zinc silicate (Li_2ZnSiO_4, Card No. 15-56) phases. The addition of small amount of In_2O_3 (0.20 mol%) in the base glass G_2 heat treated at 490 °C/5 h–745 °C/10 h (Fig. 3, pattern II, Table 2), does not lead to the formation of different phases which were obtained in the crystallized base glass G_1 (In_2O_3-free sample). However, the increase of In_2O_3 addition (0.61–1.01 mol%) in the glasses (the samples G_3 and G_4, heat treated at 495 °C/5 h–755 °C/10 h and 510 °C/5 h–765 °C/10 h respectively) led to the crystallization of pyroxene like phase, such as lithium indium silicate ($LiInSi_2O_6$, Card No. 33-0799) together with α-quartz, lithium disilicate, wollastonite and lithium zinc silicate (Fig. 3, patterns III-IV, Table 2).

The X-ray diffraction analysis (Fig. 4, pattern II) revealed that, at low addition of iron oxide (1.04 mol%) in In_2O_3-containing glasses G_5, heat-treated at 505 °C/5 h–760 °C/10 h, wollastonite containing-iron was developed together with lithium zinc silicate, α-quartz, lithium disilicate and lithium indium silicate phases, and no other iron-containing phase could be detected (Fig. 4, pattern II). However, the increase of Fe_2O_3 content in the glass up to 1.73 mol% (the sample G_6, crystallized at 485 °C/5 h–740 °C/10 h), led to the formation of ferrobustamite phase ($(Ca_{0.79}Fe_{0.21})SiO_3$, Card No. 71-0758), instead of wollastonite phase, together with lithium zinc silicate, α-quartz, lithium disilicate and lithium indium silicate phases while, wollastonite phase could not be identified (Fig. 4, pattern III).

The microstructure of the glass-ceramics was investigated by scanning electron microscopy. SEM of the fractured surface shows the effects of adding In_2O_3 and Fe_2O_3 on the microstructure of the prepared glass-ceramics (Fig. 5). SEM of the crystallized base glass G_1 (without In_2O_3 and Fe_2O_3), showed that volume crystallization of dendritic-like growths were formed (Fig. 5a).

Table 2. The crystalline phases developed in the studied glass-ceramics

Sample	Heat-treatment [°C/h]	Crystalline phases formed
G_1	480/5–745/10	α-Quartz (SiO_2) + LS_2 ($Li_2Si_2O_5$) + Wo ($CaSiO_3$) + LZS (Li_2ZnSiO_4)
G_2	490/5–745/10	α-Quartz + LS_2 + Wo + LZS
G_3	495/5–755/10	α-Quartz + LS_2 + Wo + LZS + LInS ($LiInSi_2O_6$)
G_4	510/5–765/10	α-Quartz + LS_2 + LZS + Wo + LInS
G_5	505/5–760/10	LZS + α-Quartz + LS_2 + Wo (containing iron) + LInS S
G_6	485/5–740/10	LZS + α-Quartz + F.bus. ($(Ca_{0.79}Fe_{0.21})SiO_3$) + LS_2 + LInS

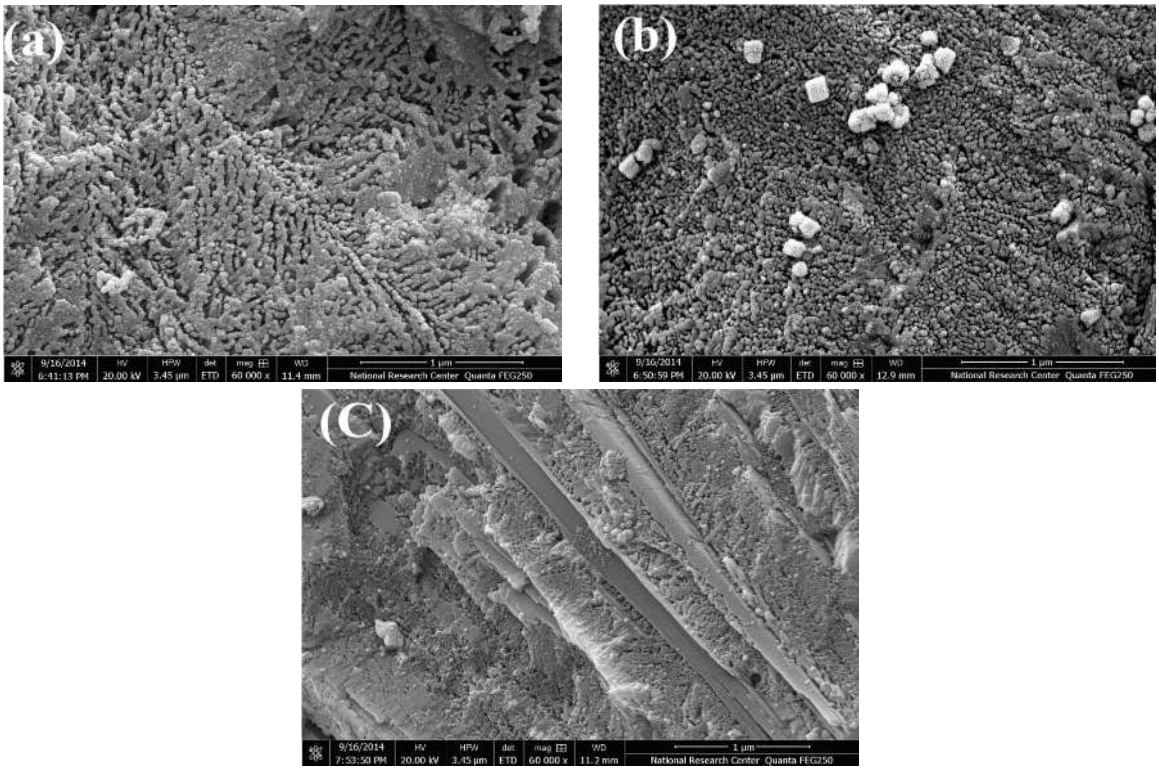

Figure 5. SEM micrograph of fracture surface of glass-ceramics: a) G_1 crystallized at 480 °C/5 h–745 °C/10 h, b) G_4 crystallized at 510 °C/5 h–765 °C/10 h and c) G_6 crystallized at 485 °C/5 h–740 °C/10 h

However, the addition of In_2O_3 in the glass composition led to form a volume crystallization of fine grained-like growths (Fig. 5b), and ultra-fine microstructure was obtained by adding iron oxide in the In_2O_3 containing glass-ceramic sample (Fig. 5c).

3.2. Thermo-mechanical properties

The measurements of the coefficients of thermal expansion (α) of the studied glass-ceramic materials were carried out in the temperature range 25–700 °C. The obtained data are graphically represented in Fig. 6. The obtained data clearly indicated that the thermal expansion coefficients decreased from 191×10^{-7} 1/°C to 150×10^{-7} 1/°C (in the temperature range 25–700 °C) when In_2O_3 was added in the glass compositions (the samples G_2-G_4). Also, the additions of iron oxide in In_2O_3-containig glass (the glass-ceramic samples G_5 and G_6) led to decrease the α-values of the resultant crystalline materials from 141×10^{-7} 1/°C to 115×10^{-7} 1/°C in the temperature range 25–700 °C (Fig. 6).

The Vickers' microhardness was determined for all prepared glass-ceramics and the obtained results are presented in Fig. 7. The microhardness values of the investigated samples are ranging from 3.56 to 5.44 GPa. The lowest microhardness value has the base crystalline sample G_1 (Fig. 7) and the additions of In_2O_3 or Fe_2O_3 in the glass compositions led to increase the microhardness values of the investigated crystalline products (Fig. 7).

IV. Discussion

4.1. Crystallization – DTA analysis

The increase in both T_g and T_c temperatures with increasing the In_2O_3 content in Zn-bearing glass (Fig. 1) may be related to the increase in coherence of the glass which consequently leads to less mobility of the structural elements in the glass structure and strengthening the glass network structure [18]. The increase of the temperature needed for the crystallization process was expected. The results also showed that the additions of Fe_2O_3 in the In_2O_3-containing glass have significant effects on lowering the T_g and T_c temperatures (Fig. 2). The number of non-bridging oxygen (NBO) increased with increasing the Fe_2O_3 content in the glasses, such increase led to decrease the temperature of endothermic peaks, i.e. a low energy is needed to induce crystallization. Li *et al.* [19] reported that iron oxide acted as a flux and phase-separation accelerator during melting. Fayon *et al*. [20–23] stated that Fe^{3+} ions are expected to occupy both tetrahedral and octahedral local sites positions in the glass network. Both of these Fe^{3+} sites formed the linkages of Si–O–Fe and In–O–Fe type. The divalent iron ions are expected to occupy only interstitial positions and act as modifiers, similar to lithium ions, depolymerizing the glass network by creating more bonding defects and non-bridging oxygens (NBO) [24]. The FeO_4 tetrahedral had a negative charge and hence required cations like Li^+ ions for charge compensation.

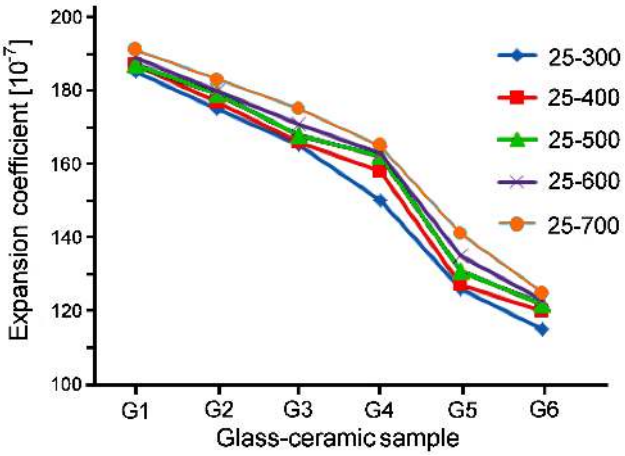

Figure 6. The coefficients of thermal expansion of the investigated glass-ceramics

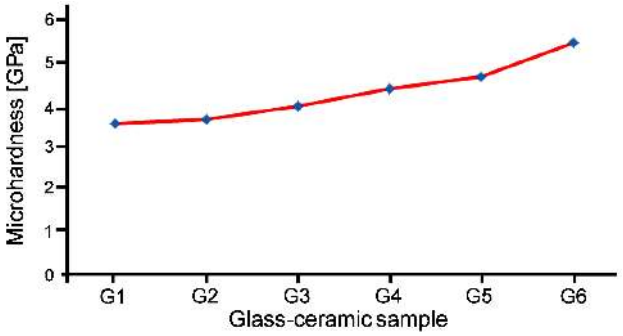

Figure 7. Vickers' microhardness of the investigated glass-ceramics

4.2. Crystallization – XRD data

The XRD patterns of the glass-ceramics showed the formation of various crystalline phases (Figs. 3 and 4). The type and proportions of the various crystalline phases in the prepared thermally treated glasses were markedly dependent on the composition of the parent glass and heat treatment applied. The X-ray diffraction analysis (Fig. 3, Pattern I) indicated that α-quartz, lithium disilicate, wollastonite and lithium zinc silicate were developed as being major phases from the base glass G_1. West and Glasser [7,8] examined the stable and metastable phase relations in the Li_2O-ZnO-SiO_2 system depending on the composition. They found that, lithium disilicate, lithium metasilicate, lithium zinc silicate and silica can be present as being major phases in this type of glass-ceramics. These phases are characterized by their high or moderately high thermal expansion coefficients making the glass-ceramic suitable for seals. Salman *et al.* [25] reported that, in the LiO_2-ZnO-SiO_2 system, Li_2ZnSiO_4 phase was developed due to the reaction of ZnO with $Li_2Si_2O_5$. The formation of lithium disilicate (LD) is preceded by the crystallization of lithium metasilicate (LS). First, lithium metasilicate crystallizes in the glass at temperatures in the range of 650–700 °C and then reacts with SiO_2 to form LD at higher temperatures.

The XRD analysis (Fig. 3, Pattern II) revealed that no In_2O_3-containing phases could be identified in the sample G_2 with low In_2O_3 addition (0.2 mol%), however, the pyroxene member of $LiInSi_2O_6$ phase crystallized as a result of increasing In_2O_3 content up to 0.61 mol% (Fig. 3, Pattern III). Further increase of In_2O_3 addition up to 1.01 mol% (the sample G_4) led to increase the crystallization of lithium indium pyroxene phase together with α-quartz, lithium disilicate, wollastonite and lithium zinc silicate (Fig. 3, Pattern IV). The present results suggest that the increase of In_2O_3 content enhances the development of $LiInSi_2O_6$ phase of pyroxene-type.

The state of iron, its coordination and concentration in the glasses mainly determined the nature of the phases formed [26,27]. The iron content has a great influence on the oxidation state of iron oxide in glass-ceramic. The ferrous cations occupy only octahedral sites which are increased in the low iron-content compositions [28]. At low Fe_2O_3 addition (1.04 mol%) in In_2O_3-containing glass G_5 lithium zinc silicate, α-quartz, lithium disilicate, wollastonite and lithium indium silicate phases predominantly crystallized and no Fe_2O_3-containing phases could be detected. However, the displacement of the major characteristics d-spacing lines of wollastonite phase towards higher 2θ values was observed. This may support the suggestion that the Fe^{2+} was incorporated in wollastonite open structure [29] and that wollastonite containing-iron could be formed. On increasing Fe_2O_3 content (1.73 mol%) in the glass composition (the sample G_6) wollastonite molecules captured more Fe^{2+} in its structure and converted to ferrobustamite $(Ca_{0.79}Fe_{0.21})SiO_3$ phase (Fig. 4, Pattern III, Table 2). This ferrobustamite phase has a pyroxenoid triclinic structure, very similar to that of β-wollastonite-($CaSiO_3$) [29]. A miscibility gap between wollastonite and ferrobustamite was discovered by Shimazaki and Yamanaka [30]. They suggested that ferrobustamite with iron content larger than that of $(Ca_{5/6}Fe_{1/6})SiO_3$ will be stable at lower temperatures, probably 300–600 °C.

4.3. Crystallization – SEM study

The microstructure of glass-ceramics is very important and determines suitable mechanical properties [31]. Scanning electron microscope revealed that the grain microstructures were changed from volume crystallization of dendritic-like growths, in the sample G_1, without In_2O_3 or Fe_2O_3, (Fig. 5a) to fine microstructure in G_4, with In_2O_3, (Fig. 5b) or, ultra-fine microstructure in G_6, with In_2O_3 and Fe_2O_3, (Fig. 5c). This is attributed to the fact that the co-crystallization of multi phases in the glass-ceramic led to form fine microstructure [4]. The variations of temperature during the heat treatment of the glass-ceramic formation also considered. The presence of iron oxide in the glasses increases the crystallization centers and stimulates the crystallization of the glass during the reheating process giving rise to volume crystallization of medium to fine grained microstructure [27].

4.4. Properties – Thermal expansion coefficient

The properties of the Zn-containing glasses are depending greatly on their composition which governs in turn the glass structure [32]. Properties of their crystalline phases are also affected by the structure, type and composition of the phases developed during crystallization process and by the originating of residual glassy matrix. The amount of the different crystalline phases is greatly important for optimizing the properties of glasses, which influences the thermo-mechanical properties of the glass-ceramics [11].

Glass-ceramics are remarkable due to very wide range of thermal expansion coefficients which can be obtained. At one extreme, there are materials having zero or even negative coefficients of thermal expansion, while, at the other extreme, materials having expansion coefficient close to those of useful metals are also available [33]. It is generally agreed that properties, such as the coefficient of thermal expansion, depend on the nature and volume of the precipitated phases, as well as the heat-treatment history [4]. Changes in the composition of the basic glass, say, substitution between different mental ions, always play a very important role in the amendment of the thermal expansion coefficient.

The thermal expansion coefficients of the investigated glass-ceramics after heat treatment are ranged from 191×10^{-7} 1/°C to 115×10^{-7} 1/°C in the temperature range 25–700 °C (Fig. 6). Lithium zinc silicate glasses generally crystallized to produce crystal phases such as lithium zinc orthosilicate (LZS) which have α-values $(110–180)\times10^{-7}$ 1/°C (25–1030 °C) [11]. While, the α-value of wollastonite is 94×10^{-7} 1/°C (100–200 °C) [34], lithium disilicate is 110×10^{-7} 1/°C (20–600 °C) [6] and α-quartz is 237×10^{-7} 1/°C (20–600 °C) [6]. According to the previous consideration, it follows therefore that, the decrease in the α-values of the studied glass-ceramics containing In_2O_3 in comparison to the crystalline sample G_1 (without In_2O_3) could be attributed to the formation of $LiInSi_2O_6$ phase having relatively low expanding coefficients [6,35]. The obtained data are in agreement with the previous results published by Salman and Salama [36], confirming that the crystallization of lithium indium silicate ($LiInSi_2O_6$) phase gives low thermal expansion coefficient of the glass-ceramic.

The addition of Fe_2O_3 in the glass composition (the samples G_5 and G_6) led to decrease in the thermal expansion coefficient values compared to the sample G_4 without Fe_2O_3. This may be due to the incorporation of iron oxide in the wollastonite structure and formation of solid solution in the form of ferrobustamite ($(Ca_{0.79}Fe_{0.21})SiO_3$) instead of wollastonite phase. However, there is no available data about the α-value of ferrobustamite phase. Glass compositions crystallizing in form of solid solutions should be of importance from the point of view of improvement the physical properties of the material [37]. Matsueda [38] reconfirmed that ferrobustamite is distinct from wollastonite in optical and chemical properties as well as cell dimensions, and considered paragenetic relations between ferrobustamite and wollastonite. The structure variation due to Ca-Fe substitution in the ferrobustamite solid solution is reflected in its cell parameter [39]. Since thermal expansion of cation polyhedra is in general geometrically similar to the expansion due to cation substitution, thermal expansion of the cation octahedra in ferrobustamite would be expected to impose a similar rotation effect upon silicate tetrahedral.

From the obtained data, it is clear that the difference in content and type of crystal phases formed in the evaluated crystalline solid samples may lead to differences in their thermal expansion coefficients (Fig. 7). Salman and Mostafa [40] pointed out that the presence of iron oxide increases the number of crystallization centres and stimulates the crystallization of the glass during the reheating process, giving to rise volume crystallization of medium to fine grained textures. Thus, the increase of crystal content is advantageous in reducing the linear thermal expansion coefficient and improving the thermal stability [41]. The degree of crystallization might also have a significant influence on the thermal expansion coefficient [42].

4.5. Properties – Microhardness

Hardness, defined as the material resistance to localized deformation, is an important mechanical property of materials. Hard materials have many industrial applications wherever resistance to abrasion and wear are important [43]. The hardness of glass-ceramic is related to both crystalline and residual glassy phases. The changes of the crystalline phases with temperature certainly affect the physical properties of the glass-ceramics [44].

Hardness of glass-ceramics is proportional to its wear resistance. The microhardness values of the glass-ceramic samples are presented in Fig. 7. The reported data (3.56–5.44 GPa) showed that, the modification of the glass composition by adding In_2O_3 and Fe_2O_3 enable formation of glass-ceramic materials with good mechanical properties. The reason might be the formation of finer grains microstructure than those formed in the base crystalline sample G_1 (without In_2O_3 and Fe_2O_3) as indicated from the SEM micrographs (Fig. 5).

The microhardness of glass-ceramics generally increased with the increase of the crystallization tendency, smaller crystalline grains as well as formation of fine microstructure [45]. The presence of iron ions in glass-ceramics (the samples G_5 and G_6), that served as nucleation accelerator, enhanced the crystallization process and this promoted internal melt precipitation of the crystal [46]. Under certain conditions, the formation of more crystal nuclei decreases the growth rate of single crystals, leading to finer crystal grains (Figs. 5b,c). Song *et al.* [47] reported that the amount of crystal particles increases when the size decreases which is followed with a reduction in the content of the glass phase. These all make the structure more compact, and can meet the requirements of wear resistance in the glass-ceramic.

V. Conclusions

The contributions of In_2O_3 and Fe_2O_3 to the crystallization of the glasses based on Li_2O-ZnO-CaO-SiO_2 system have been studied. The developed crystalline phases after controlling heat treatments were α-quartz (SiO_2), lithium zinc silicate (Li_2ZnSiO_4), wollastonite ($CaSiO_3$), lithium disilicate-($Li_2Si_2O_5$), wollastonite containing-iron, ferrobustamite ($(Ca_{0.79}Fe_{0.21})SiO_3$) and lithium indium silicate ($LiInSi_2O_6$) phases. The thermal expansion coefficient and microhardness of the corresponding glass-ceramics were also measured. The obtained results showed that the α-values of the crystalline products, in the temperature range 25–700 °C, decreased from 191×10^{-7} 1/°C to 115×10^{-7} 1/°C by addition of In_2O_3 and Fe_2O_3. While Vickers' microhardness values of the glass-ceramics increased from 3.56 to 5.44 GPa with addition of In_2O_3 and Fe_2O_3. Thus, the incorporation of indium and iron oxides in varying concentrations improved the mechanical properties and the thermal stability in the resultant glass-ceramics.

References

1. L.R. Pinckney, G.H. Beal, "Microstructural evolution in some silicate glass-ceramics: A review", *J. Am. Ceram. Soc.*, **91** (2008) 773–779.
2. X. Zheng, G. Wen, L. Song, X.X. Huang, "Effects of P_2O_5 and heat-treatment on crystallization and microstructure in lithium disilicate glass-ceramics", *Acta Mater.*, **56** (2008)549–558.
3. G. Nagarjuna, N. Venkatramaiah, P.V.V. Satyanarayana, N. Veeraiah, "Fe_2O_3-induced crystallization and the physical properties of lead arsenate glass system", *J. Alloys Comp.*, **468** (2009) 466–472.
4. W. Holand, G.H. Beall, *Glass-Ceramic Technology*, The American Ceramics Society, Westerville, OH, USA, 2002.
5. I.W. Donald, B.L. Metcalfe, D.J. Wood, J.R. Copley, "The preparation and properties of some lithium zinc silicate glass-ceramics", *J. Mater. Sci.*, **24** (1989) 3892–3903.
6. P.W. McMillan, *Glass-Ceramics*, Academic Press, London, New York, 1979.
7. A.R. West, F.P. Glasser, "Crystallization of lithium zinc silicates, Part I. Phase equillibria in the system Li_4SiO_4-$ZnSiO_4$", *J. Mater. Sci.*, **5** (1970) 557–565.
8. A.R. West, F.P. Glasser, "Crystallization of lithium zinc silicates, Part II. Comparison of the metastable and stable phase relations and the properties of the lithium zinc orthosilicates", *J. Mater. Sci.*, **5** (1970) 676–688.
9. Z.X. Chen, P.W. McMillan, "Crystallization behaviour of a high zinc content Li_2O-ZnO-SiO_2 glass-ceramics and the effect of K_2O additions", *J. Am. Ceram. Soc.*, **68** [4] (1985) 220–224.
10. I.W. Donald, B.L. Metcalfe, A.E.P. Morris, "Influence of transition metal oxide additions on the crystallization kinetics, microstructures and thermal expansion characteristics of a lithium zinc silicate glass", *J. Mater. Sci.*, **27** (1992) 2979–2999.
11. B.I. Sharma, M. Goswami, P. Sengupta, V.K. Shrikhande, G.B. Kale, G.P. Kothiyal, "Study on some thermo physical properties in Li_2O-ZnO-SiO_2 glass-ceramics", *Mater. Lett.*, **58** (2004) 2423–2428.
12. M. Goswami, P. Sengupta, K. Sharma, R. Kumar, V.K. Shrikhande, J.M.F. Ferreira, "Crystallization behaviour of Li_2O-ZnO-SiO_2 glass-ceramics system", *Ceram. Int.*, **33** (2007) 863–867.
13. P.F. James, "Glass-ceramics: new compositions and uses", *J. Non-Cryst. Solids*, **181** (1995) 1–15.
14. A.X. Lu, Z.B. Ke, Z.H. Xiao, X.F. Zhang, X.Y. Li, "Effect of heat-treatment condition on crystallization behavior and thermal expansion coefficient of Li_2O-ZnO-Al_2O_3-SiO_2 glass-ceramics", *J. Non-Cryst. Solids*, **353** (2007) 2692–2697.
15. M. Goswami, S.K. Deshpande, R. Kumar, G.P. Kothiyal, "Electrical behaviour of Li_2O-ZnO-SiO_2 glass and glass-ceramics system", *J. Phys. Chem. Solids*, **71** (2010) 739–744.
16. Y. Zhang, Z. Luo, T. Liu, X. Hao, Z. Li, A. Lu, "MgO-doping in the Li_2O-ZnO-Al_2O_3-SiO_2 glass-ceramics for better sealing with steel", *J. Non-Cryst. Solids*, **405** (2014) 170–175.
17. P. Mingying, Q. Jianrong, C. Danping, M. Xiangeng, Z. Congshan, "Broadband infrared luminescence from Li_2O-Al_2O_3-ZnO-SiO_2 glasses doped with Bi_2O_3", *Optics Express*, **13** (2005) 6892–6898.
18. X. Jun, X. Zi-Fan, Z. Wei-Hong, L. Ye, C. Jin-Shu, "The effect of Al_2O_3/SiO_2 on the structure and properties of Na_2O-CaO-Al_2O_3-SiO_2 glasses", *Key Eng. Mater.*, **509** (2012) 339–345.
19. W. Li, H. Luo, L. Jianan, L. Jiazhi, J. Guo, "Studies on the microstructure of the black-glazed bowl sherds excavated from the Jian kiln site of ancient China", *Ceram. Int.*, **34** (2008) 1473–1480.
20. F. Fayon, C. Bessada, D. Massiot, I. Farnan, J.P. Coutures, "29Si and 207Pb NMR study of local order in lead silicate glasses", *J. Non-Cryst. Solids*, **232** (1998) 403-408.
21. P.J. Bray, M. Leventhal, H.O. Hooper, "Nuclear magnetic resonance investigations of the structure of lead borate glasses", *Phys. Chem. Glasses*, **4** (1963) 47–66.
22. P.A. Bingham, J.M. Parker, T.M. Searle, I. Smith, "Local structure and medium range ordering of tetrahedrally coordinated Fe^{3+} ions in alkali-alkaline earth-silica glasses", *J. Non-Cryst. Solids*, **353** (2007) 2479–2494.
23. M.M. El-Desoky, F.A. Ibrahim, M.Y. Hassaan, "Effect of sulfur addition on the transport properties of semiconducting iron phosphate glasses", *Solid State Sci.*, **13** (2011) 1616–1622.
24. P. Ramesh Babu, R. Vijay, V. Ravi Kumar, D. Krishna Rao, N. Veeraiah, "The influence of In_2O_3 on electrical characteristics of iron mixed Li_2O-PbO-B_2O_3-SiO_2-Bi_2O_3 multi-component glass system",

Ceram. Int., **40** (2014) 8311–8322.
25. S.M. Salman, H. Darwish, E.A. Mahdy, "The influence of Al_2O_3, MgO and ZnO on the crystallization characteristics and properties of lithium calcium silicate glasses and glass-ceramics", *Mater. Chem. Phys.*, **112** (2008) 945–953.
26. C.R. Kurkjian, E.A. Sigety, "Coordination of Fe^{3+} in glass", *Phys. Chem. Glasses*, **9** (1968) 73–83.
27. S.M. Salman, S.N. Salama, "Pyroxene solid solution crystallized from CaO-MgO (Li_2O,Fe_2O_3)-SiO_2 glasses", *Ceram. Int.*, **12** (1986) 221–228.
28. M. Romero, J.M. Rincon, A. Acosta, "Effect of iron oxide content on the crystallization of a diopside glass-ceramic glaze", *J. Eur. Ceram. Soc.*, **22** (2002) 883–890.
29. W.A. Deer, R.A. Howie, J. Zussman, *An Introduction to the Rock-Forming Minerals*, Third ELBS impression, Hong Kong, Common Wealth, Printing Press Ltd., 1992.
30. H. Shimazaki, T. Yamanaka, "Iron wollastonite from skarns and its stability relation in the $CaSiO_3$-$CaFeSiO_6$ join", *Geochem. (Japan)*, **7** (1973) 67–79.
31. J. Henry, R.G. Hill, "The influence of lithia content on the properties of fluorphlogopite glass-ceramics, II-Microstructure hardness and machineability", *J. Non-Cryst. Solids*, **319** (2003) 13–30.
32. H.A. Abo-Mosallam, H. Darwish, S.M. Salman, "Crystallization characteristic and properties of some zinc containing soda lime silicate glasses", *J. Mater. Sci.: Mater. Electron.*, **21** (2010) 889–896.
33. B. Aitken, G.H. Beall, "Glass-Ceramics" pp. 269–294 in *Materials Science and Technology, Vol. 11, Structure and Properties of Ceramics*, Eds. R.W. Cahn, P. Haasen, E.J. Kramer, VCH, Weinheim, Germany, 1994.
34. Z. Strnad, "Glass-ceramic materials", pp. 195-252 in *Glass Science and Technology*, Vol. 8, Elsevier, Amsterdam, the Netherlands, 1986.
35. M. Cameron, S. Sueno, C.T. Prewitt, J.J. Papike, "High-temperature crystal chemistry of acmite, diopside, hedenbergite, jadeite, spodumene and ureyite", *Am. Mineral.*, **58** (1973) 594–618.
36. S.M. Salman, S.N. Salama, "Crystallization and thermal expansion characteristics of In_2O_3-containing lithium iron silicate-diopside glasses", *Ceramics-Silikáty*, **55** (2011) 114–122.
37. P.S. Rogers, "The initiation of crystal growth in glasses", *Mineral. Mag.*, **37** (1970) 741–758.
38. H. Matsueda, "Immiscibility gap in the system $CaSiO_3$-$CaFeSi_2O_6$ at low temperatures", *Mineral. J. (Japan)*, **7** (1974) 327–343.
39. T. Yamanaka, R. Sadanaga, Y. Takeuchi, "Structural variation in the ferrobustamite solid solution", *Am. Mineral.*, **62** (1977) 1216–1224.
40. S.M. Salman, F. Mostafa, "Crystallization of alkali-iron-borosilicate glasses", *Sprechsaal*, **118** (1985) 622–676.
41. C. Ye, F. He, H. Shu, H. Qi, Q. Zhang, P. Song, J. Xie, "Preparation and properties of sintered glass-ceramics containing Au-Cu tailing waste", *Mater. Design*, **86** (2015) 782–787.
42. A. Karamanov, M. Pelino, M. Salvo, I. Metekovits, "Sintered glass-ceramics from incinerator fly ashes, Part II. The influence of the particle size and heat-treatment on the properties", *J. Eur. Ceram. Soc.*, **23** (2003) 1609–1615.
43. M.A. Caravaca, L.E. Kosteski, J.C. Mino, R.B. Ambra, B. Uberti, R.A. Casali, "Model for Vickers microhardness prediction applied to SnO_2 and TiO_2 in the normal and high pressure phases", *J. Eur. Ceram. Soc.*, **34** (2014) 3791–3800.
44. B. Mirhadi, B. Mehdikhani, N. Askari, "Effect of zinc oxide on microhardness and sintering behaviour of MgO-Al_2O_3-SiO_2 glass-ceramic system", *Solid State Sci.*, **14** (2012) 430–434.
45. F.J. Torres, J. Alarcon, "Mechanism of crystallization of pyroxene based glass-ceramic glazes", *J. Non-Cryst. Solids*, **347** (2004) 45–51.
46. H. Yang, C. Chen, L. Pan, "Preparation of double-layer glass-ceramic/ceramic tile from bauxite tailings and red mud", *J. Eur. Ceram. Soc.*, **29** (2009) 1887–1894.
47. L. Song, J. Wu, Z. Li, X. Hao, Y. Yongsheng, "Crystallization mechanisms and properties of α-cordierite glass-ceramics from K_2O-MgO-Al_2O_3-SiO_2 glasses", *J. Non-Cryst. Solids*, **419** (2015) 16–26.